

Field-induced Bose-Einstein Condensation of triplons up to 8 K in $\text{Sr}_3\text{Cr}_2\text{O}_8$ A. A. Aczel,¹ Y. Kohama,² C. Morosan,³ F. W. Eickert,⁴ M. Jaime,² O. E. Ayala-Valenzuela,²
R. D. McDonald,² S. D. Selesnic,¹ H. A. Dabkowska,⁵ and G. M. Luke^{1,5,6}¹Department of Physics and Astronomy, McMaster University, Hamilton, Ontario, Canada, L8S 4M1²National High Magnetic Field Laboratory, Los Alamos National Laboratory, Los Alamos, New Mexico 87545, USA³CEA-Grenoble, Institut Nanosciences et Cryogenie, SP5M-S-LATEQS,
17 rue des Martyrs, 38054 Grenoble Cedex 9, France⁴Max Planck Institute for Chemical Physics of Solids, Dresden, Germany⁵Brockhouse Institute for Materials Research, McMaster University, Hamilton, Ontario, Canada, L8S 4M1⁶Canadian Institute of Advanced Research, Toronto, Ontario, Canada, M5G 1Z8

(Dated: February 22, 2024)

Single crystals of the spin dimer system $\text{Sr}_3\text{Cr}_2\text{O}_8$ have been grown for the first time. Magnetization, heat capacity, and magnetocaloric effect data up to 65 T reveal magnetic order between applied fields of $H_{c1} = 30.4$ T and $H_{c2} = 62$ T. This field-induced order persists up to $T_c^{\text{max}} = 8$ K at $H = 44$ T, the highest observed in any quantum magnet where H_{c2} is experimentally-accessible. We fit the temperature-field phase diagram boundary close to H_{c1} using the expression $T_c = A(H - H_{c1})^\beta$. The exponent $\beta = 0.65(2)$, obtained at temperatures much smaller than T_c^{max} , is that of the 3D Bose-Einstein condensate (BEC) universality class. This finding strongly suggests that $\text{Sr}_3\text{Cr}_2\text{O}_8$ is a new realization of a triplon BEC where the universal regimes corresponding to both H_{c1} and H_{c2} are accessible at ^4He temperatures.

PACS numbers: 73.43.Nq, 75.30.Kz, 75.30.Sg, 75.40.Cx

The Bose-Einstein condensate (BEC) is a unique state of matter in which a macroscopic number of bosons collapse into a global (identical) quantum state[1, 2]. Although superfluid ^4He [3] is possibly the most studied BEC system, ultracold Rb gas proved to be the first true experimental realization of this exotic state of matter[4]. Since the original discovery was made, other BECs have been identified in optical lattices, superconductors[5], and optically-pumped magnon gases[6] where the phenomenon of BEC can be studied at room temperature.

Giamarchi and Tsvelik first showed that the Hamiltonians of quantum antiferromagnets and BECs were directly related by a mapping transformation[6], following up on earlier work by Matsubara and Matsuda[7]. Although real lattices always have imperfections and symmetry-breaking terms, in some materials these can be neglected since they only affect their properties below the experimentally-accessible window. This then suggests that a very good approximation to a BEC can be achieved in solid-state magnetic systems. In particular, spin dimer systems were perceived to be good candidates to display BEC behaviour. These systems exhibit spin-singlet ground states with a spin gap to the first excited triplet state. This gap can be closed by applying a large enough magnetic field, resulting in the generation of a macroscopic number of triplet excitations (triplons). If the kinetic energy terms dominate the potential energy terms in the U(1) invariant Hamiltonian of such a system, the resulting ground state can be described as a BEC.

TiCuCl_3 was the first spin dimer system to show evidence for a triplon BEC ground state[8, 9], and this has stimulated a flurry of research in triplon BECs[10, 11, 12, 13, 14]. Currently, the primary goal is to search

for systems displaying BEC behaviour in the space of externally-controlled parameters completely accessible in the laboratory. This allows the associated quantum phase transitions to be studied experimentally.

The field-induced order in a triplon BEC is nothing but the well-known XY-AFM (easy-plane antiferromagnetic) state. Such a system can either be visualized as a lattice gradually filling with hard-core triplons, or as an XY-AFM where the in-plane component of the canted spins varies from zero in the paramagnetic state, to a maximum at approximately midway between H_{c1} and H_{c2} , to zero again in the fully-polarized state. The external control parameter in both cases is the applied magnetic field, and the order parameter is the number of triplons or, equivalently, the magnitude of the staggered moment M_{xy} . The (H, T) phase boundary in ideal 3D systems follows the expression $T_c = A(H - H_c)^{2/3}$ close to the critical fields H_{c1} and H_{c2} . Symmetry breaking terms can affect real systems by changing the universality class from XY-AFM (easy plane) to Ising (easy axis), in which case the critical exponent changes from $2/3$ to $1/2$, or by changing the dimensionality of the system [15].

In this letter, we present the first evidence for a BEC ground state in the spin dimer system $\text{Sr}_3\text{Cr}_2\text{O}_8$ through a combination of high field magnetization ($M(H)$), heat capacity, and magnetocaloric effect (MCE) measurements. This is one of a series of isostructural spin dimer compounds with the general formula $A_3M_2O_8$ [16, 17, 18] where $A = \text{Ba}$ or Sr and $M = \text{Cr}$ or Mn . These compounds crystallize in the $R\bar{3}m$ space group at room temperature, and the magnetic M^{5+} ions are tetrahedrally-coordinated with O^{2-} ions. The M^{5+} ions may carry spins of either $S = 1/2$ or 1, and as a result of having

only one nearest neighbour (NN) magnetic ion they form spin dimers along the c -axis. While the A^{2+} ions are essentially isolated from the MO_4 tetrahedra, they seem to play an important role in controlling the NN $M-M$ distance and the value of the associated spin gap. For example, while $Ba_3Cr_2O_8$ has a NN $Cr-Cr$ distance of 3.9765 Å and a spin gap of 15.6(3) K [19], $Sr_3Cr_2O_8$ has a smaller NN $Cr-Cr$ distance of 3.842 Å and hence a larger spin gap of 61.9(1) K [18]. This is consistent with the expectation that a smaller NN distance between the magnetic ions should yield a larger antiferromagnetic intradimer exchange interaction. The stronger intradimer exchange interaction in the $Sr-Cr$ system pushes the temperature scale of the magnetic order to the highest values observed yet in a system where H_{c2} is experimentally-accessible.

Single crystals of $Sr_3Cr_2O_8$ were grown by the optical coating zone method at McMaster University. We first mixed together stoichiometric quantities of $SrCO_3$ and Cr_2O_3 . The resulting powder was shaped into 10–12 cm long rods, which were annealed for 72 hours in air at 1200 °C and then quenched to room temperature. The rods cracked during the annealing process, so they were remade following this and subsequently annealed for 5 hours in high purity Ar gas at 1200 °C to strengthen them for the coating zone growths. Since $Sr_3Cr_2O_8$ is congruently melting in Ar gas, the crystals were grown at a very high rate of 20 mm/h with an Ar pressure of 170 kPa and a temperature of 1470 °C. The phase purity of the resulting crystals was confirmed by powder x-ray diffraction, and they were aligned by Laue x-ray diffraction.

The anisotropy of the g -factor was measured via electron paramagnetic resonance (EPR) at 70 GHz using a resonant cavity mounted in a cryogenic goniometer, so as to rotate the sample and resonant environment in situ. The temperature was maintained at 30 K to ensure sufficient thermal population of the triplet state using a 4He flow cryostat. The magnetic field was applied using a superconducting solenoid and calibrated using the conventional EPR marker DPPH. The g -factors were found to be $g_c = 1.938(6)$ and $g_{ab} = 1.950(1)$.

Fig. 1 depicts dc susceptibility measurements of our crystals. At high temperatures, the data follow a Curie-Weiss law. Below 40 K, the susceptibility decreases sharply with decreasing temperature, which is characteristic of non-magnetic spin-singlet ground state systems. The susceptibility measurements also reveal that this system is nearly isotropic. We fit the susceptibility data to an interacting dimer model of the form:

$$\chi = \frac{N_A (\mu_B g)^2}{k_B T (3 + \exp(J_0/T) + J'/T)} + \chi_0 + \frac{A}{T} \quad (1)$$

where N_A is Avogadro's number, μ_B is the Bohr magneton, J_0 is the intradimer exchange constant, and J' is the sum of the interdimer exchange constants. The last two terms represent contributions from Van Vleck paramagnetism/core diamagnetism and impurity/defect

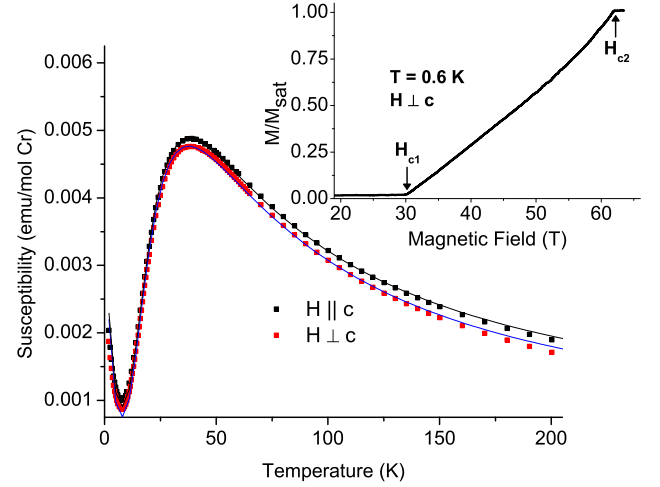


FIG. 1: (color online) dc susceptibility measurements of $Sr_3Cr_2O_8$ with an applied field of 1 T. The data was fit to an isolated dimer model. The inset shows the magnetization $M(H)$ as measured in a 65 T short pulse magnet.

spins respectively. We fixed the g -factors in the fits to the values obtained by EPR. From the fitting, we found only 0.8% free $S = 1/2$ moments, and estimated the exchange constants to be $J = 61.5(3)$ K and $J' = 12(2)$ K. Note that the latter are actually best determined by inelastic neutron scattering [20].

Magnetization data was collected using an extraction magnetometer in conjunction with a 3He fridge and a 65 T short pulse (35 ms) magnet at the National High Magnetic Field Laboratory (NHMFL) in Los Alamos, New Mexico. The Fig. 1 inset shows $M(H)$ for the $H \parallel c$ orientation while sweeping the field up. $M(H)$ has a very small value up to $H_{c1} = 30.4$ T due to defects/impurities in the sample. Above $H_{c1} = 30.4$ T, the spin gap is closed resulting in a magnetically-ordered regime between H_{c1} and $H_{c2} = 62$ T where $M(H)$ increases roughly linearly with H . Finally, above H_{c2} $M(H)$ saturates as the system reaches the fully-polarized state.

To further characterize the field-induced order, heat capacity and MCE measurements were performed using a home-built calorimeter [12, 21]. These measurements were conducted in a 3He fridge placed in the core of a 35 T resistive magnet at the NHMFL in Tallahassee, Florida. The MCE data was collected for the $H \parallel c$ orientation, sweeping the field both up and down at 3 T/min. The quasi-adiabatic MCE yields a sharp change in the sample temperature when entering or leaving a magnetically-ordered state to ensure entropy conservation [22].

Fig. 2 (a) shows a color contour plot of the entropy as a function of temperature and field. S was calculated from the MCE data using the equation:

$$S = \int_{T_{bath}}^T \frac{C_p}{T} dt \quad (2)$$

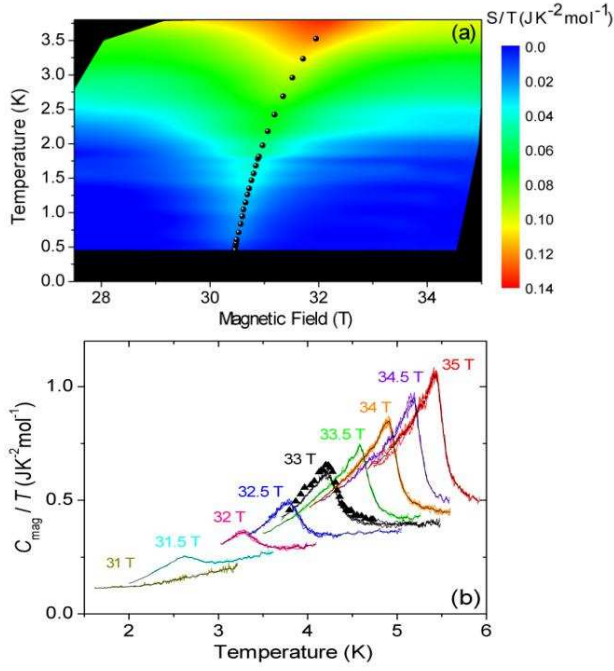


FIG. 2: (color online) (a) Color contour plot of the entropy S/T of $\text{Sr}_3\text{C}_2\text{O}_8$, as calculated from the MCE data. The phase boundary determined by MCE is shown with black dots. (b) Selected heat capacity data as obtained by the dual slope method. For 33 T, data was also collected by the standard relaxation method (black triangles).

where κ is the thermal conductivity of the thermal link in the calorimeter, T is the sample temperature, and T_{bath} is the bath temperature. We measured κ as a function of T at both 0 and 33 T and found very little difference in the two curves, so the 33 T thermal conductivity data was used in all our calculations. The absolute entropy was then obtained by a calibration process using 31.5 T heat capacity data. We chose to plot S/T to improve the contrast since the entropy associated with the transition drops quickly with decreasing temperature. As one crosses the phase boundary at a constant temperature, a peak in the entropy is clearly evident. This results because both the low-field gapped phase and the ordered phase above the transition should have small entropies. However, in the proximity of the transition we likely have fluctuations of the order parameter characteristic of a second order transition and hence a much higher entropy.

Heat capacity measurements are presented in Fig. 2(b) for the $H \parallel \hat{c}$ orientation. The majority of the data was collected using the dual slope method with a large ΔT [23]. The main advantage of this technique is that data can be collected quickly which is important for efficient use of power in high field resistive magnets. However, this often comes at a cost of reduced accuracy, and so data is generally collected for at least one applied field using the standard relaxation technique to compare the two methods directly. In the present case, this was done at

33 T (black triangles in Fig. 2(b)). The excellent agreement between the techniques suggests that the dual slope method estimates the heat capacity well in $\text{Sr}_3\text{C}_2\text{O}_8$.

The emergence of a lambda-like anomaly was clearly observed with an increasing applied field beyond $H_{c1} = 30.4$ T; this provides unambiguous evidence for the field-induced order in this system. The lambda anomaly is small for fields close to H_{c1} , but becomes much more prominent with increasing applied field as seen in Fig. 2(b). Heat capacity data was also collected for the $H \parallel \hat{a}$ orientation. Similar lambda anomalies were observed in that case, and the transition temperatures were systematically shifted down by only 0.2 K for a given applied field. This indicates that $\text{Sr}_3\text{C}_2\text{O}_8$ is a very isotropic, as previously suggested by the susceptibility measurements.

The spin gap in $\text{Sr}_3\text{C}_2\text{O}_8$ is quite large, and so DC fields provided by resistive magnets can access only a very small region of the phase diagram. For this reason, we also performed MCE measurements in both the 50 T mid-pulse (300 ms) and 60 T long-pulse (2 s) magnets in Los Alamos. For these measurements, a tiny $\text{Sr}_3\text{C}_2\text{O}_8$ single crystal ($200 \times 100 \times 50 \text{ } \mu\text{m}^3$) was inserted into a small, home-built calorimeter [24]. To the best of our knowledge, these were the first successful MCE experiments performed in a pulsed field facility.

Fig. 3 presents a phase diagram for the $H \parallel \hat{c}$ orientation of $\text{Sr}_3\text{C}_2\text{O}_8$ as obtained from our specific heat, MCE and $M(H)$ experiments. The asymmetric nature of the dome is quite unusual for a triplon BEC system; further studies are required to understand this feature. From the heat capacity measurements, the ordering temperature for a given field was taken as the peak of the lambda-like feature. From the MCE data, the ordering temperature for a given field was determined by locating the extrema in the first derivative of the sample temperature with respect to field [2, 21]. Some selected up-sweep MCE curves are superimposed on the phase diagram. For clarity reasons we show only one down-sweep MCE curve; the sample temperature changes in the opposite manner to the up-sweep data near the transition as expected. No irreversible/dissipative mechanisms typical for a first order phase transition were observed. Many MCE scans were completed at low temperatures so it would be possible to determine a critical exponent. The fitted data all must lie in the universal regime for the obtained critical exponent to be meaningful, and an earlier Monte Carlo simulation study [25] suggested that the universal regime extends no higher than $0.4 T_c^{\text{max}}$, where T_c^{max} is the maximum temperature of the magnetically-ordered regime. In the present case, we have determined that the top of the dome lies around 8 K. To ensure that we stayed within the universal regime, only the MCE data below 2.7 K was fit to a power law of the form: $T_c = A(H - H_{c1})$.

Although one can perform a three parameter fit, H_{c1} and A are not independent variables. For this reason, we resorted to a series of two parameter fits where H_{c1} was

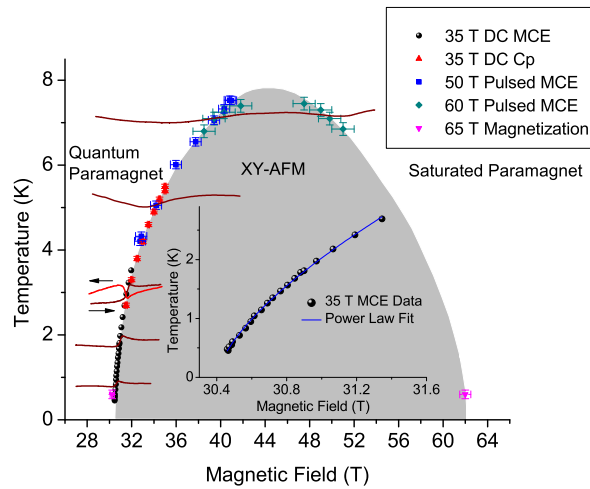


FIG. 3: (color online) $\text{Sr}_3\text{Cr}_2\text{O}_8$ phase diagram with selected MCE traces superimposed and the ordered region shaded as a guide to the eye. Due to small temperature changes at the transitions, the MCE traces have been magnified. The inset shows the result of fitting the data near H_{c1} to a power law.

systematically fixed at different values and was determined from the fitting. Our best fit yielded $\beta = 0.65(2)$ with a corresponding $H_{c1} = 30.40(1)$ T. The former is in agreement with the expected value of $2/3$ for a 3D BEC universality class, strongly suggesting that $\text{Sr}_3\text{Cr}_2\text{O}_8$ is a realization of a new triplon BEC.

Finally, let us comment here on the nature of the magnetically-ordered state in $\text{Sr}_3\text{Cr}_2\text{O}_8$. The spin structures in the ordered states of the isostructural systems $\text{Ba}_3\text{Cr}_2\text{O}_8$ [13] and $\text{Ba}_3\text{Mn}_2\text{O}_8$ [21] have both been determined previously, and the results were quite different. In the case of $\text{Ba}_3\text{Mn}_2\text{O}_8$, a combination of single ion anisotropy and geometric frustration lead to both an incommensurate spiral spin phase and an Ising-type modulated structure in the ordered regime [21]. The shape and structure of the phase diagram for that material depends on the orientation of the system relative to the applied field. In sharp contrast, neutron measurements revealed a commensurate, collinear spin structure in $\text{Ba}_3\text{Cr}_2\text{O}_8$ [13]. This is likely a result of the geometric frustration being relieved due to a structural distortion courtesy of a co-operative Jahn-Teller effect [26]. A similar Jahn-Teller effect has been reported for $\text{Sr}_3\text{Cr}_2\text{O}_8$ [27], suggesting that the spin structure of the ordered state is very similar to the case of $\text{Ba}_3\text{Cr}_2\text{O}_8$.

In summary, we have determined the full (H, T) phase diagram for $\text{Sr}_3\text{Cr}_2\text{O}_8$ from both thermodynamic measurements and high-field magnetization. This phase diagram provides direct evidence for field-induced order in this system between $H_{c1} = 30.4$ T and $H_{c2} = 62$ T, with an unprecedented maximum ordering temperature $T_C^{\text{max}} = 8$ K. The phase boundary near H_{c1} was fitted to a power law. Our obtained critical exponent of $0.65(2)$

agrees with the 3D BEC universality class, and so this strongly suggests that $\text{Sr}_3\text{Cr}_2\text{O}_8$ is a realization of a new triplon BEC system. Since a large portion of the universal regime in this material can be accessed via ^3He systems, both the H_{c1} and H_{c2} quantum critical regimes can be studied in detail. This may help us to understand the asymmetric nature of the phase diagram and other more general aspects of triplon BEC phenomena. Note that no experimental criticality studies near H_{c2} have been reported for triplon BEC systems to-date.

We acknowledge useful discussions with C.D. Batista and technical/experimental assistance from A.B. Dabkowski, F. Balakirev, and N. Harrison. Research at McMaster University is supported by NSERC and CIFAR. Research at NHMFL is supported by the National Science Foundation, the Department of Energy, and the State of Florida.

-
- [1] E.A. Comella and C.E. Williams, *Rev. Mod. Phys.* **74**, 875 (2002).
 - [2] W. Ketterle, *Rev. Mod. Phys.* **74**, 1131 (2002).
 - [3] A.F.G. Wyatt, *Nature* **391**, 56 (1998).
 - [4] L.P. Pitaevskii and S. Stringari, *Bose-Einstein Condensation*, Clarendon Press, Oxford (2003).
 - [5] S.O. Demokritov et al., *Nature* **443**, 430 (2006).
 - [6] T. Giamarchi and A.M. Tsvelik, *Phys. Rev. B* **59**, 11398 (1999).
 - [7] T. Matsubara and H. Masuda, *Prog. Theo. Phys.* **16**, 569 (1956).
 - [8] A. Oosawa et al., *J. Phys. Cond. Matt.* **11**, 265 (1999).
 - [9] T. Nikuni, M. Oshikawa, A. Oosawa, and H. Tanaka, *Phys. Rev. Lett.* **84**, 5868 (2000).
 - [10] M. Jaime et al., *Phys. Rev. Lett.* **93**, 087203 (2004).
 - [11] V.S. Zapf et al., *Phys. Rev. Lett.* **96**, 077204 (2006).
 - [12] A.A. Czele et al., *Phys. Rev. B* **79**, 100409(R) (2009).
 - [13] M. Kofu et al., *Phys. Rev. Lett.* **102**, 177204 (2009).
 - [14] S.E. Sebastian et al., *Nature* **441**, 617 (2006).
 - [15] For a recent review, see: T. Giamarchi, C. Ruegg, and O. Tchernyshyov, *Nature Physics* **4**, 198 (2008).
 - [16] T. Nakajima, H. Mita, and Y. Ueda, *J. Phys. Soc. Jpn.* **75**, 054706 (2006).
 - [17] M. Uchida, H. Tanaka, M. J. Bartashevich, and T. Goto, *J. Phys. Soc. Japan* **70**, 1790 (2001).
 - [18] Y. Singh and D.C. Johnston, *Phys. Rev. B* **76**, 012407 (2007).
 - [19] A.A. Czele, H.A. Dabkowska, P.R. Provencher, and G.M. Luke, *J. Cry. Growth* **310**, 870 (2008).
 - [20] D. Quintero-Castro et al., *arXiv:0909.3941* (unpublished).
 - [21] E.C. Samulon et al., *Phys. Rev. B* **77**, 214441 (2008).
 - [22] A.V. Silhanek et al., *Phys. Rev. Lett.* **96**, 136403 (2006).
 - [23] S.R. Jegel and G.W. Weber, *J. Phys. E: Sci. Instrum.* **19**, 790 (1986).
 - [24] Y. Kohama, C. Maroenat, and M. Jaime, in preparation.
 - [25] N. Kawashima, *J. Phys. Soc. Japan* **73**, 3219 (2004).
 - [26] M. Kofu et al., *Phys. Rev. Lett.* **102**, 037206 (2009).
 - [27] L.C. Chapon, C. Stock, P.G. Radaelli, and C. Martin, *arXiv:0807.0877* (unpublished).